NIST Internal Report
NIST IR 8521

Predicting Heat Release Rate from Fire Video Data

Part 1. Application of Deep Learning Techniques

Kuldeep Prasad

This publication is available free of charge from:
https://doi.org/10.6028/NIST.IR.8521

NIST Internal Report
NIST IR 8521

Predicting Heat Release Rate from Fire Video Data

Part 1. Application of Deep Learning Techniques

Kuldeep Prasad
Fire Research Division
Engineering Laboratory

This publication is available free of charge from:
https://doi.org/10.6028/NIST.IR.8521

May 2024

U.S. Department of Commerce
Gina M. Raimondo, Secretary

National Institute of Standards and Technology
Laurie E. Locascio, NIST Director and Under Secretary of Commerce for Standards and Technology

NIST IR 8521
May 2024

Publication History
Approved by the NIST Editorial Review Board on 2024-05-01

How to Cite this NIST Technical Series Publication
Kuldeep Prasad (2024) Predicting Heat Release Rate from Fire Video Data. 1. Application of Deep Learning Techniques (National Institute of Standards and Technology, Gaithersburg, MD), NIST Series (NIST IR 8521) Publication ID. https://doi.org/10.6028/NIST.IR.8521

Author ORCID iDs
Kuldeep Prasad: 0000-0002-5817-7306

Contact Information
kprasad@nist.gov

Abstract

A novel approach for estimating transient heat release rate from fire images and video using deep learning techniques is presented. The heat release rate (HRR) is a critical parameter in characterizing the fire hazard and thermal effects of a burning item. It is an effective indicator of the fire growth rate and fire hazard that is used extensively in building fire safety design. However, for outdoor fires, heat release rate measurements are usually not available due to lack of measurement equipment.

The goal of this work is to develop and demonstrate a novel technique based on “image calorimetry” for predicting heat release rate using video data and recurrent neural network models. The proposed methodology only requires video camera data and can be extended to outdoor fire experiments. Results of the trained neural network model on the investigated set of experiments conducted in a laboratory setting, show excellent comparison between predicted and temporally evolving heat release rate measurements, with an overall accuracy score of 0.94.

Keywords

Data Intensive Research; Deep Learning; Fire Calorimetry Database; Fire Heat Release Rate; Wildland Urban Interface.

Table of Contents

List of Tables

List of Figures

Author 1: Conceptualization, Methodology, Software, Writing.

1. Introduction

The fire heat release rate (HRR) is considered one of the more critical parameter in characterizing the behavior of a fire and thermal effects of a burning item. It is an effective indicator of the fire growth rate and fire size that is used extensively in both building fire safety design and fire research [1]-[5]. However, for outdoor fires, heat release rate data is not available due to lack of calorimetric techniques suitable for this environment. Conventional techniques for estimating HRR and the challenges in using these methods for outdoor fires are discussed in the following sub-sections, followed by the overall goals for this report.

1.1. Measuring Heat Release Rate inside a laboratory

Conventionally, the fire HRR is measured in a laboratory through two principal approaches:

1) measuring the fuel mass burning rate and

2) oxygen consumption calorimetry.

For fuels whose heat of combustion (ΔH_C) is known, the burning rate ($\dot{m}_f$) can be measured using a mass balance (non-gaseous fuels) or using a flow rate meter (gaseous fuels). Then the HRR can be calculated as:

$$\boldsymbol{HRR = \dot{m}_f \eta \Delta H_C} \tag{1}$$

where ΔH_C is the heat of combustion in units of kJ/kg, and η is the combustion efficiency. Major issues with this method however, are that the values of ΔH_C and η are unknown for complex fuel.

Oxygen consumption calorimetry for estimating HRR is more widely used for fires and fuels of different scales. Assuming a constant heat of oxidation for most common fuels, and complete combustion, the HRR of an arbitrary fuel is given by

$$\boldsymbol{HRR = \Delta \dot{m}_{O_2} \Delta H_{O_2}} \tag{2}$$

where $\Delta \dot{m}_{O_2}$ is the oxygen consumption in a fire in units of kg/s, and ΔH_{O_2} is the heat generated per unit mass of oxygen consumed in units of kJ/kg. The heat of oxidation ΔH_{O_2} is assumed constant at 13.1 MJ/kg, regardless of fuel. The oxygen consumption can be measured if the experiment is performed in a controlled laboratory setting under an exhaust hood [6]. Equation 2 can then be used to estimate the heat release rate of the fire. However, many fire tests are too large to be performed under a conventional hood. The capacity of the hood may sometimes limit the size of the experiments that can be safely conducted inside a laboratory. Other fire experiments may corrode the sensitive measurement equipment or may produce toxic gases that can make it unsuitable for indoor laboratory testing.

There are other scenarios such as wind driven fire experiments, such as wildland-urban interface (WUI) prescribed burns, which cannot be performed in a controlled laboratory setting, and hence, these experiments do not have access to a hood for oxygen calorimetry. For such scenarios, it is very difficult to estimate the time dependent heat release rate. Furthermore, the time dependent heat release rate is often prescribed as an input parameter in a Computational Fluid Dynamics (CFD) fire model; the lack of reliable heat release rate data makes it difficult to conduct numerical simulations of the fire event. There is clearly a need for an accurate methodology for estimating HRR for outdoor fires.

1.2. Empirical Methods for estimating Heat Release Rate

For an axisymmetric fire source, the flame height can be estimated using the Heskestad correlation [7], expressed as follows:

$$\boldsymbol{L/D = 3.7\,\dot{Q}^{*2/5} - 1.02} \tag{3}$$

where, L represents the flame height, D is the flame diameter and $\dot{Q}^*$ is the non-dimensional heat release rate, defined as follows:

$$\dot{Q}^* = \frac{\dot{Q}}{\rho_\infty c_p T_\infty \sqrt{g\,D^5}}$$

Here, ρ_∞ is the ambient density (kg/m^3), c_p is the specific heat of air at constant pressure (kJ/kg/K), T_∞ is the ambient temperature (K), and g is acceleration due to gravity (m/s^2).

The Heskestad correlation Eq. (3) can be inverted to obtain the heat release rate $\dot{Q}$, as shown below:

$$\dot{Q} = \left[\left(\frac{1}{0.235}\frac{L}{D} + 4.34\right)D\right]^{2.5} \tag{4}$$

The equation above relates the heat release rate (kW) to the flame height L (m) and flame diameter D (m). Assuming that the temporally varying flame height and flame diameter are known or can be estimated from an image or a video of an experiment, this equation can be used to predict the heat release rate of a fire.

Appendix A presents a case study of estimating heat release rate using the Heskestad's correlation for a simple calorimetry confirmation burner experiment. It is demonstrated that estimating flame length and flame diameter accurately from images can be challenging and can result in large errors in the estimated HRR. Similar conclusions have been made by other authors [8]-[15]. There is clearly a need for a more robust method to estimate heat release rate, especially for outdoor fires.

Orloff & DeRis [16] related the transient heat release rate of a fire to its temporally evolving volume, as shown below:

$$\dot{Q} = \gamma\,V(t)$$

For steady pool fires, the proportionality constant parameter γ was estimated to be 1200 kW/m^3, while for highly turbulent jet, the volume term was raised to power of 1.11. Estimating the temporally evolving flame volume is a challenging task from fire video data. As a result, estimating HRR using the above equation is quite challenging as well.

The goal of this report is to develop a methodology for estimating the heat release rate of a fire by using its recorded video data and deep learning techniques. There are a few publications [8], [9], [17]-[21] that make use of video recordings to estimate flame height and heat release rate. Omiotek and Kotyra [18] combined flame image processing with a deep convolutional neural network for identifying undesired combustion states. Bonner et. al [19] presented an algorithm for estimating the fire volume using two cameras, located at an approximately right angle to each other. They subsequently used the temporally evolving volume to estimate the heat release rate of turbulent jet fires. Wang et. al [20] used convolution neural networks to estimate heat release rate. They used single images for estimating heat release rate instead of the entire video data. They [21] also proposed the use of stereo camera and deep learning to estimate the distance between the fire and the camera.

Evans et. al [22] attempted to correlate the heat release rate of the 1991 Kuwait oil field fires to their flame height. The total heat release rate of a fire is composed of two parts: a convective heat release rate fraction and a radiative heat release rate fraction. Sivathanu and Gore [23] have shown in laboratory studies that the radiant heat flux can be used to estimate the total radiative heat release rate fraction of jet flames.

1.3. Goals for this report

In this report we develop and demonstrate a novel technique based on “image calorimetry”, to estimate heat release rate from fire video data and deep learning technique. This new technique is dependent on the availability of video data which is usually readily available for both indoor and outdoor fires. We demonstrate that the methodology can be used to predict heat release rate for indoor as well as outdoor fires.

In comparison, conventional techniques such as those based on oxygen consumption calorimetry requires equipment that is not available for outdoor fires. Similarly, mass loss rate measurements for outdoor fires can result in large errors, especially in the presence of ambient wind. Table 1 provides a summary of the scenarios where conventional techniques cannot be used for estimating heat release rate. Table 1 also indicates that “image calorimetry” method can be used both inside and outside the laboratory, with or without ambient wind, since it is only dependent on the availability of video data.

The impact of this work is the development and demonstration of a novel technique "image calorimetry", for estimating the heat release rate for outdoor fires with or without ambient wind, where conventional techniques fail to provide HRR measurements.

Table 1. Comparison of conventional techniques for estimate HRR with Image Calorimetry technique

	Heat Release Rate Oxygen Calorimetry	Mass Loss Rate	Image Calorimetry (current approach)
Inside Laboratory	✓	✓	✓
Outside Laboratory		✓	✓
Outside Laboratory With Wind			✓

A deep learning model based on recurrent neural networks [24] was developed to ingest the sequential images extracted from a fire video obtained from a single camera. The model was trained on 147 experiments for which video data and HRR measured using oxygen depletion calorimetry were available. Details of the neural network model will be discussed in Section 2.

Once the deep learning model was trained, it was validated on a set of experiments that were independent of the training set. Accuracy of the predicted results were compared with measured values and the deep learning model was iteratively improved (Section 3). The goal of this research is to use the trained model on other full scale test images and videos from outdoor experiments with or without an ambient wind to predict the time varying heat release rate. Finally, in Section 4 we summarize the major conclusions of this project as well as discuss future opportunities and challenges.

2. Methods

In most fire tests or actual fire incidences, video data is often available. Wide-spread use of Closed Circuit Television (CCTV) cameras and mobile phone cameras can record the flame spread patterns and smoke movement. Data can also be obtained from airborne systems including drones as well as satellite images. The videos include information on fire behavior and characteristics, such as flame size, height, color, brightness, and oscillation frequency, as well as their time evolution. In depth evaluation of the flame images can deliver valuable information about fire development. With the development of artificial intelligence (AI) technology, especially deep learning methods, the capability of image analysis has been significantly improved. This section will develop the methodology for using fire scene images to predict the transient HRR of any burning item, with application to outdoor fires with or without ambient wind.

2.1. Fire Calorimetry Database (FCD)

AI models require large number of fire-scene images labelled with their transient HRR values for training [24]. The NIST Fire Calorimetry Database (FCD), is an online public resource [25] containing the results of fire experiments conducted at the National Fire Research Laboratory (NFRL). The FCD consists of data augmented video, images, plots as well as tabulated data from many fire experiments. Each experiment is described with metadata, time dependent calculations based on dozens of sensors, and input parameters, each with quantified uncertainty.

The Fire Calorimetry Database was adopted for training a deep learning model, which relates the fire images and video with the evolution of fire HRR from ignition to burnout, measured through oxygen consumption calorimetry. Various fire scenarios, such as single burning items, fully furnished rooms, controlled burners, well-characterized fuels, and fuels of unknown composition, with fire HRR ranging from 50-20,000 kW, are part of the Fire Calorimetry Database [25].

2.1.1. Extracting Labeled Images from Video Data

We chose to focus on experiments in the NIST FCD [25] that were part of two projects:

1) Transient Combustibles 2018
2) Multiple Item Transient Combustibles 2020.

The two projects were chosen because they included experiments on a variety of burning objects including gas burners, cardboard boxes, wood pallets and plastic cart with laptop and printer. Furthermore, the burning objects in these experiments had an aspect ratio (ratio of width to breadth) close to one, and the observed fire was mostly symmetric. This results in approximately symmetric flame shapes, where the dynamics could be reasonably captured with a single video recorder. The Transient Combustibles 2018 dataset consists of 107 experiments with peak HRR ranging between 0 - 3.1 MW. The Multiple Item Transient Combustibles 2020 dataset consisted of 41 experiments with peak HRR ranging between 0 - 4.2 MW. The duration of each experiment also varied significantly as summarized in Table 2. Images were extracted from video data of each experiment at the sampling rate indicated in Table 2.

Table 2. Datasets used for the analysis.

Dataset	# of Exp	pHRR (MW)	Duration (minutes)	# of Frames	Frame Sampling Interval (s)
Transient Combustibles 2018	107	0.0 - 3.1	3 - 103	4667	100 s, 1 s (>200kW)
Multiple Item Transient Combustibles 2020	41	0.0 - 4.2	17 - 120	8643	100 s, 5 s (>200kW)
Combined Dataset	**148**	**0.0 - 4.2**	**3 – 120**	**13310**	**100, 5, 1**

The Fire Calorimetry Database contains raw video data for each of the experiments in the two datasets, along with time dependent HRR measurements. Images were extracted from the video data along with their labels (HRR) at specific intervals as shown in Table 2. Reviewing images and labels extracted at 100s interval, indicated that we were missing the short duration high heat release rate events. More data was therefore collected at 1 s or 5 s intervals, but this was restricted to HRR values greater than 200 kW.

Some video data can include long idle period before the ignition event happens. In other cases, video data was collected well after the extinction. Image extraction was however limited to the period between the ignition and extinction, to avoid collecting large amounts of data with zero HRR value. Data collection at the two different frequencies allowed us to roughly balance the dataset with both low and high values of HRR. A total of 4667 labeled frames were collected for the 107 experiments that were part of the Transient Combustibles 2018 dataset. Similarly, we collected 8643 labeled images for the Multiple Item Transient Combustibles 2020 dataset. All images collected from the two datasets were combined, and subsequently used to train and validate the neural network models discussed in the next section.

Figure 1 shows a histogram of the heat release rate for the various frames extracted from the Multiple Item Transient Combustibles 2020 dataset. The plot shows the count of images with labels that fall within each bin of the histogram. This plot indicates that there are more frames at lower heat release rate and fewer frames at the higher heat release rate. The collected data has a small data imbalance issue, in-spite of the fact that we attempted to collect more frames at higher frequencies for the high heat release cases.

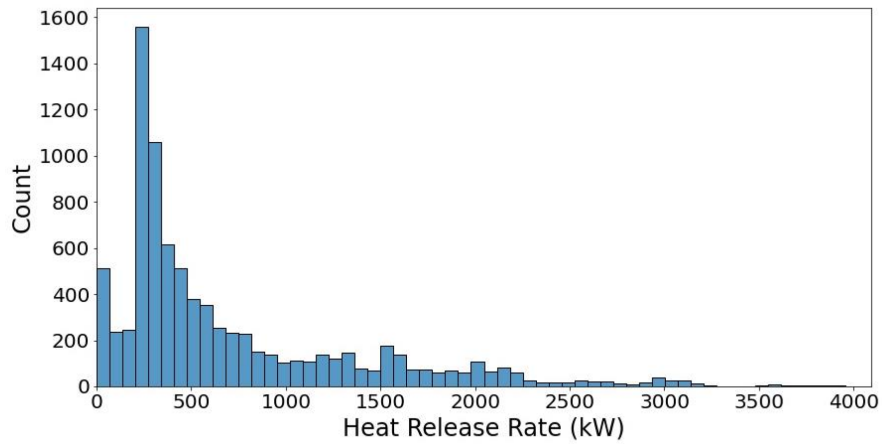

Figure 1. Histogram plot of the Heat Release Rate for the labeled images collected from the Multiple Item Combustion Calorimetry Dataset. The plot shows the count of images with labels that fall within each bin.

Figure 2 shows the number of frames extracted for each of the 41 experiments that are part of the Multiple Item Transient Combustibles 2020 dataset. The duration of the experiments in this test series varies between 17-120 minutes. This results in variability in the number of frames that were extracted from each experiment.

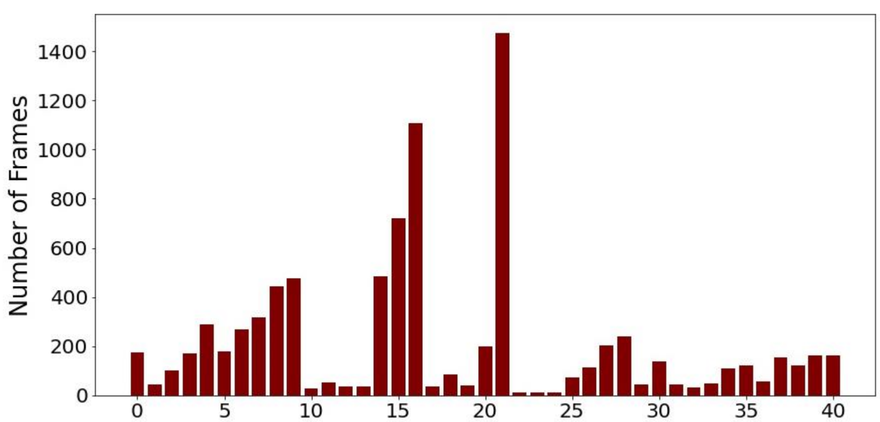

Figure 2. Number of labeled frames extracted for each of the 41 experiments that are part of the Multiple Item Combustion Calorimetry 2020 dataset.

2.1.2. Standardizing Pixel Size

The 148 experiments in this study were conducted under different hoods at the NIST National Fire Research Laboratory as seen in Table 3. The Transient Combustibles 2018 experiments were performed under the 0.5 m and 3 m hoods, while the Multiple Item Transient Combustibles 2020 experiments were performed under the 3 m and 10 m hoods. The location of the video recorder relative to the burning object also varied in these experiments. As a result, the pixel size in the images varied from one experiment to another, as summarized in Table 3. It is critical that the extracted labeled frames have a consistent pixel size. A pre-processing step was required to convert the pixel size of each image to the base (standard) pixel size. A base (standard) pixel size of 3.95 mm was chosen for pre-processing the images.

Table 3. Hood size, image shape and pixel size (mm) for the various experiments that are part of the current study

	# of Exp	# of Frames	Hood (MW)	Image Shape	pixel size (mm)
Transient Combustibles 2018	107	4667	0.5, 3	1080 x 1920 x 3	2.28, 3.71, 3.83
Multiple Item Transient Combustibles 2020	41	8643	3, 10	1080 x 1920 x 3	3.60, 3.95

When the pixel size of an image was smaller than the base pixel size, we padded the image on all four sides and then resized the image to increase the pixel size of the image. Similarly, if the pixel size of the image was larger than the base pixel size, we cropped the image on all four sides, and subsequently resized the image to decrease the pixel size. This process ensures that all the images have a consistent pixel size. The images along with their labels were pre-processed and are now in consistent format for use with neural network models, discussed in the next section.

2.2. Neural Networks for Estimating HRR

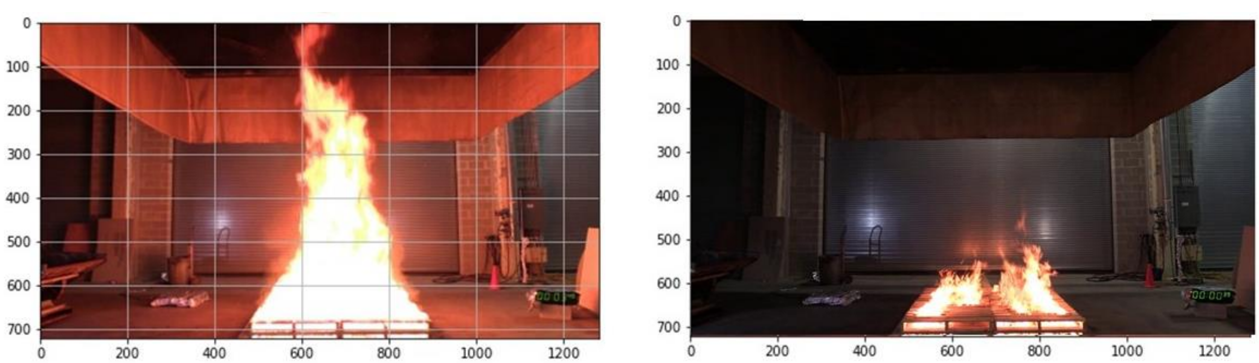

Figure 3. Image of a large fire (large HRR) on the left, and an image of smaller fire (small HRR) on the right

Figure 3 shows an image of a large fire on the left, as well as an image of a smaller fire on the right. Human beings can very quickly and accurately classify the image on the left as a large fire (large HRR), and the image on the right as a small fire (small HRR). This is because the neurons in our brain have been trained since childhood to classify fires. The training process took a long time, but now that the neurons have been fully trained, we can quickly and accurately classify fires by just looking at the images.

However, the neurons in our brain have not been taught to quantify the HRR of a fire based on a fire image. This is because they have not been exposed to appropriate data. In the next few sections, we describe an approach for constructing a neural-network model and train it on labeled image data for predicting heat release rate.

2.2.1. Challenges with Neural Networks

Computers see fire images as a collection of pixels with value ranging between 0-255. Figure 4 shows a coarse resolution image of a fire, along with pixel values superimposed on the image. Moreover, a computer does not recognize the ordering of the pixels in rows and columns. Instead, the computer flattens out the array of pixels into a single vector.

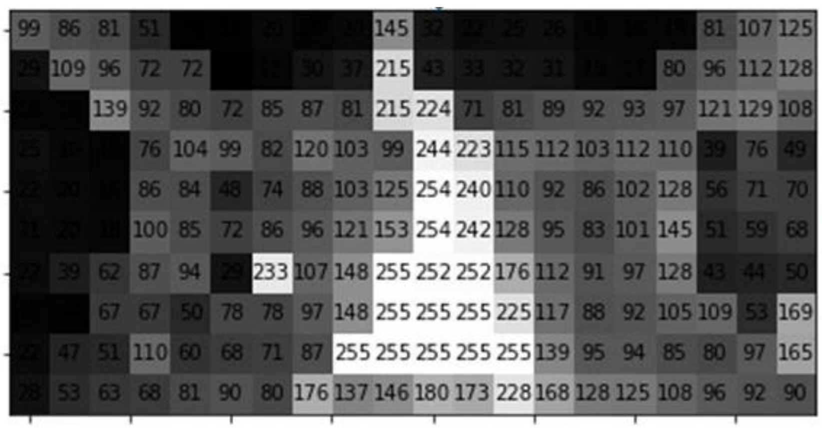

Figure 4. Coarse resolution, gray scale rendering of the fire image shown in Figure 3 (left sub-image), along with the pixel values that range between 0-255.

The challenge for a neural network model is to take this vector of numbers and quantify the HRR of the corresponding image. A human brain would not be able to process a large vector of numbers (of length ~ 6 million) as shown in Figure 4 , and quantify the HRR or even classify the image as a large fire or a small fire.

2.2.2. Processing Sequence of Images

Convolution Neural Network (CNN) models [24], [26] can take a single image and attempt to quantify the heat release rate for that image as shown schematically in Figure 5. A typical video can be broken down into a sequence of images. However, the basic Convolution Neural Network model does not take advantage of the fact that each image is part of a video. A typical Convolution Neural Network model does not know about any of the other images in the video and can be described as a static model. Such models do not maintain any context from previous images and there is no ordering of the images either.

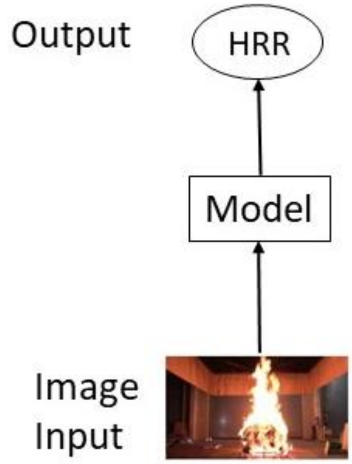

Figure 5. Convolution Neural Networks (CNN) models

2.2.3. Recurrent Neural Network (RNN)

The approach used in the current work employs a dynamic memory model [24], [26] as shown in Figure 6. The input to such a model is the entire sequence of images that are part of a video. In a dynamic memory model, a memory state is maintained to gather information from previous images of a video. As a result, the model maintains context and has information about the order of the images. We deploy a bi-directional model that keeps track of the images that came before the current image, as well as those that came after the current image.

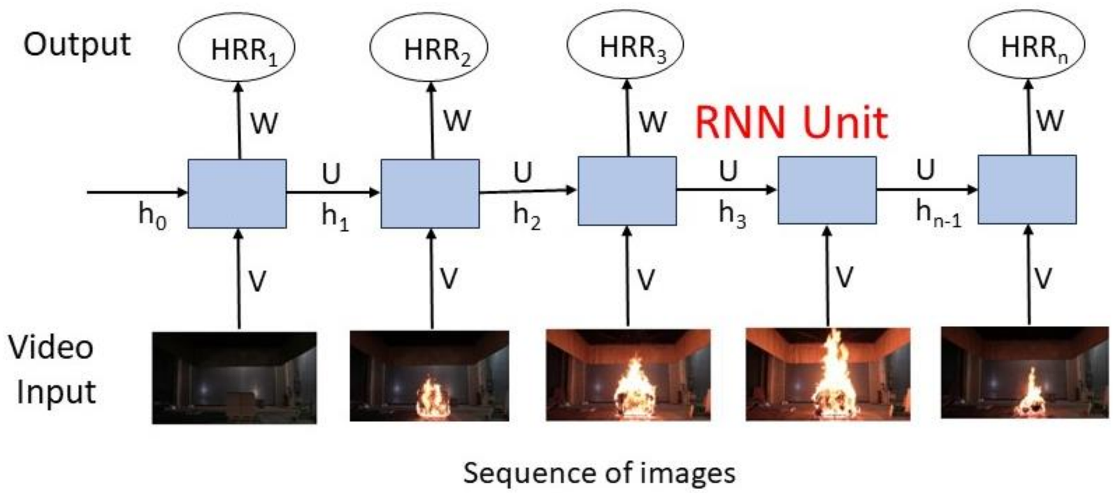

Figure 6.Recurrent Neural Network (RNN) model for analyzing video input data

The entire dataset of 148 experiments was split randomly into a training set of 118 experiments and a validation set of 30 experiments. This was accomplished through a random 80-20 train-test split. The random nature of the split does not distinguish between large fires or small fires.

The train set was used to train the Recurrent Neural Network (RNN) model shown in Figure 6. Regularization techniques such as L2, dropout as well as image augmentation techniques (translation, rotation) were used to reduce model overfitting. Once the model was trained, the validation dataset was used to test the model. Since the model has never seen the validation set during the training process, it represents a blind test for the model. We next present results from the model validation study.

3. Results and Discussion

The trained neural network model was used to predict the time dependent heat release rate of various experiments that were part of the validation set. The model has never seen the experiments that are part of the validation set, during the training process, hence the prediction on these experiments is a good measure of the validity / accuracy of the model.

3.1. Heat Release Rate of a Wood pallets and cardboard box experiment

Figure 7 (left sub-figure) shows a frame corresponding to the peak heat release rate of a fire experiment involving wood pallets and 8 cardboard boxes with paper (Exp ID 1576165873). This experiment was part of the Multiple Item Transient Combustibles 2020 dataset. A total of 1475 frames were extracted from the video of this experiment.

Figure 7 (right sub-figure) shows the time dependent measured HRR using oxygen consumption calorimetry (red solid line with symbols). The temporally evolving HRR shows a double hump profile with a peak HRR values of ~3.4 MW. The black error bars represent the uncertainty in the oxygen consumption calorimetry measurement data (see Figure 15 in reference [25]). The green dashed line represents the prediction from the RNN model.

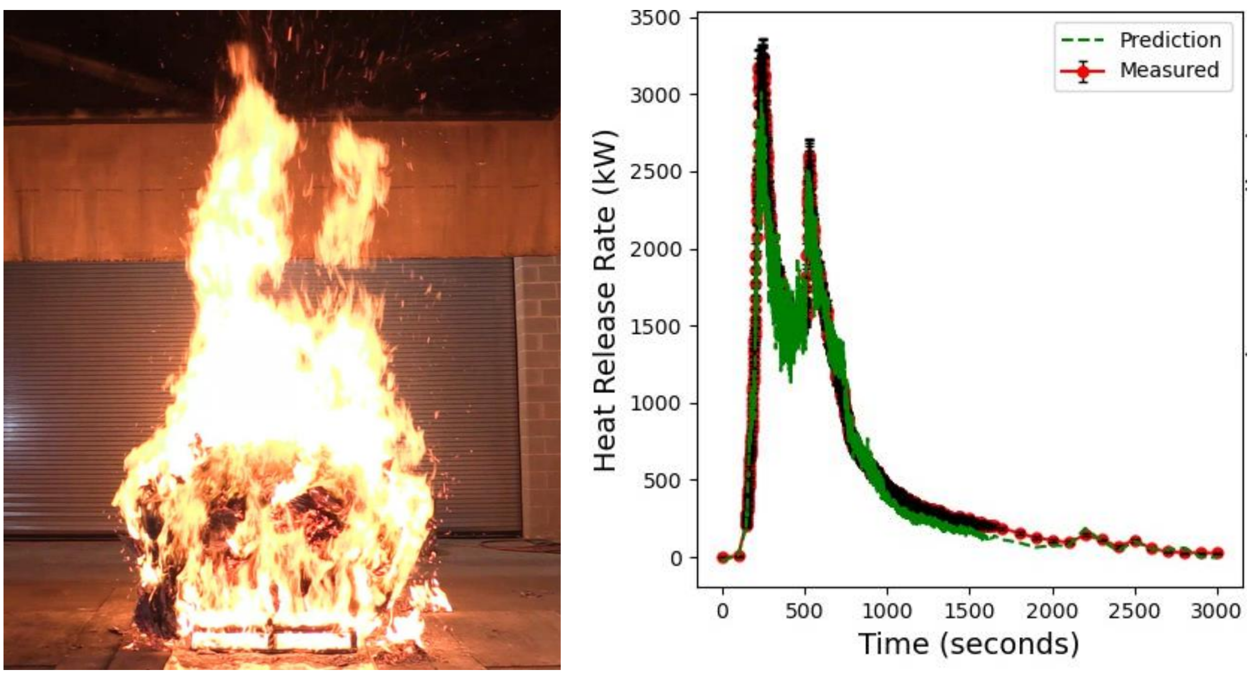

Figure 7. A trained neural network model was used to predict the time-dependent Heat Release Rate of Wood pallets and cardboard box (FCD experiment ID 1576165873) shown in the left sub-figure. The right sub-figure shows a comparison between the measured and predicted HRR values.

The neural network predictions were found to closely follow the measured HRR. Our results indicate good comparison between model predictions and measured time dependent HRR. The peak HRR is also predicted very accurately, along with the double hump profile of the HRR curve.

Table 4 provides a summary of the key results of the neural network analysis. The accuracy of the prediction as measured by an R2 score for this specific experiment was 0.95. Table 4 also provides the final model loss, mean absolute error (MAE), and the % uncertainty for the wood pallets and cardboard box experiment.

Table 4. Summary table for the wood pellets and 8 cardboard boxes with paper experiment.

# of frames	Loss	MAE (kW)	R2	% uncertainty
1475	28920	115	0.95	4.0 % PHRR

3.2. Heat Release Rate of Natural Gas Calibration Burner

This sub-section shows results for natural gas calibration burner experiment (Exp ID 1536760151) that was part of Transient Combustibles 2018 dataset. The experiment was performed with a tube gas burner, where the natural gas flow rate was adjusted to various levels during the experiment.

Figure 8 (left sub-figure) shows a frame corresponding to the peak HRR, while Figure 8 (right sub-figure) shows the time dependent measured HRR using oxygen consumption calorimetry (red solid line with symbols) during this experiment. The black error bars represent the uncertainty in the measurement data (see Figure 15 in reference [25]). The green dashed line represents the prediction from the RNN model.

The neural network predictions were found to closely follow the measured HRR. Our results indicate good comparison between model predictions and measured time dependent HRR. Table 5 provides a summary of the key results of the neural network analysis. The accuracy of the prediction as measured by an R2 score was 1.0 for this experiment. Table 5 also provides the final model loss, mean absolute error (MAE), and the % uncertainty for the natural gas calibration burner experiment.

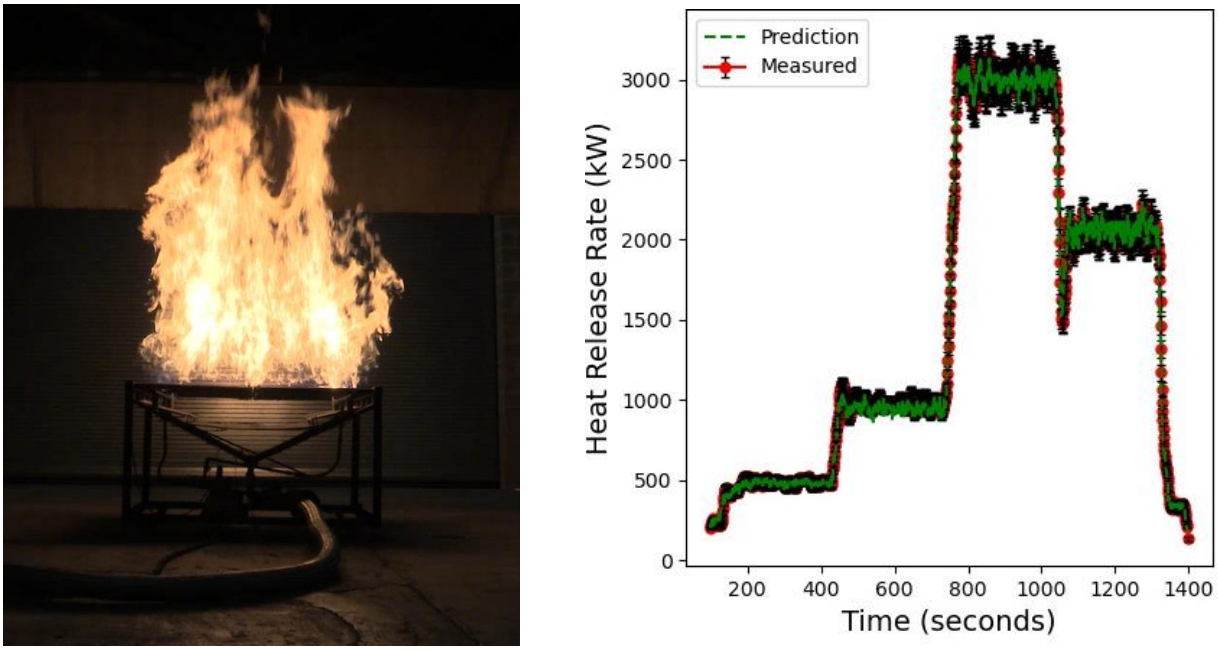

Figure 8. A trained neural network model was used to predict the time-dependent Heat Release Rate of a Natural Gas Calibration Burner experiment (FCD experiment ID 1536760151) shown in the left sub-figure. The right sub-figure shows a comparison between the measured and predicted HRR values.

Table 5. Summary table for the calibration burner experiment.

# of frames	Loss	MAE (kW)	R2	% uncertainty
1297	2126	33	1.0	4.0 % PHRR

3.3. Heat Release Rate for all the experiments - Summary

Figure 9 shows a comparison of model predicted HRR (kW) values and experimental measurements for all the 13310 frames that were extracted from the 148 experiments. The training set experiments are shown in blue, while the validation set experiments are shown in orange. The red dotted line represents the 1:1 line. A perfect model would have all the data points aligned with the 1:1 line. Results indicate that the neural network model predictions are well correlated with the measurement data.

Each of 13310 data points on this plot represents a frame that was obtained from the video data. Figure 10 shows the same data along with uncertainty bars in the measurement data. For this plot, the measurement uncertainty was also used for the model predictions error. Results indicate that the neural network model was able to learn the complex relationship between the video data and the HRR measurements. Results for the validation experiments also lie along with red dotted 1:1 line.

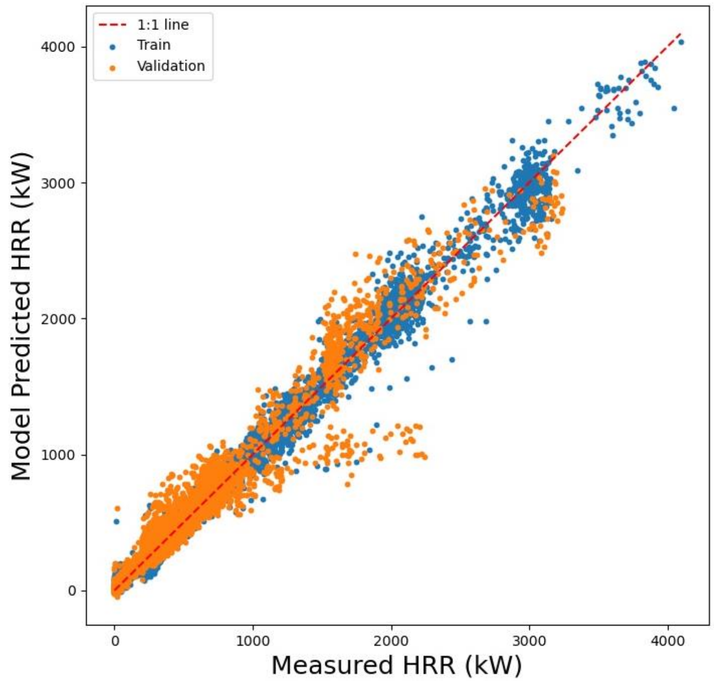

Figure 9. Comparison of model predicted and measured HRR for the 13310 frames that were extracted from the 147 fire experiments. Results indicate that the neural network model predictions are well correlated with the measurement data. The dotted red line represents the 1:1 line.

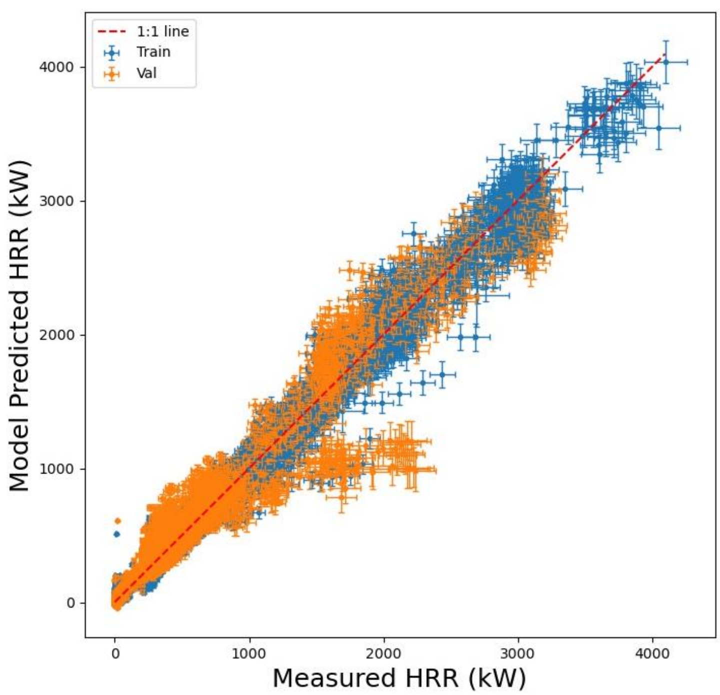

Figure 10. Comparison of model predicted and measured HRR, including error bars for the 13310 frames that were extracted from the 147 fire experiments. Results indicate that the neural network model predictions are well correlated with the measurement data. The dotted red line represents the 1:1 line.

A few frames that are part of the validation set are seen to diverge away from the 1:1 line in Figure 10. These frames are highlighted by a red circle in the left sub-figure of Figure 11. All of these frames came from a single experiment in the validation set. This experiment (ExpID 1536596869) involved the burning of a work cart with laptop and printer. During this experiment, the fire started on the top level of the work cart, which resulted in melting of the plastic. As the fire progresses, dripping was observed, and a liquid pool formed on the lower level of the work cart. Subsequently, the pool on the lower level ignited as well, the top-level collapsed, followed by burning of the entire cart until all the combustibles were consumed. This is a rather unique experiment in the validation set, and the neural network model did not have the opportunity to learn from a similar experiment in the training set. Removing this experiment from the validation set, increased the R2 score on the validation set from 0.94 to 0.96.

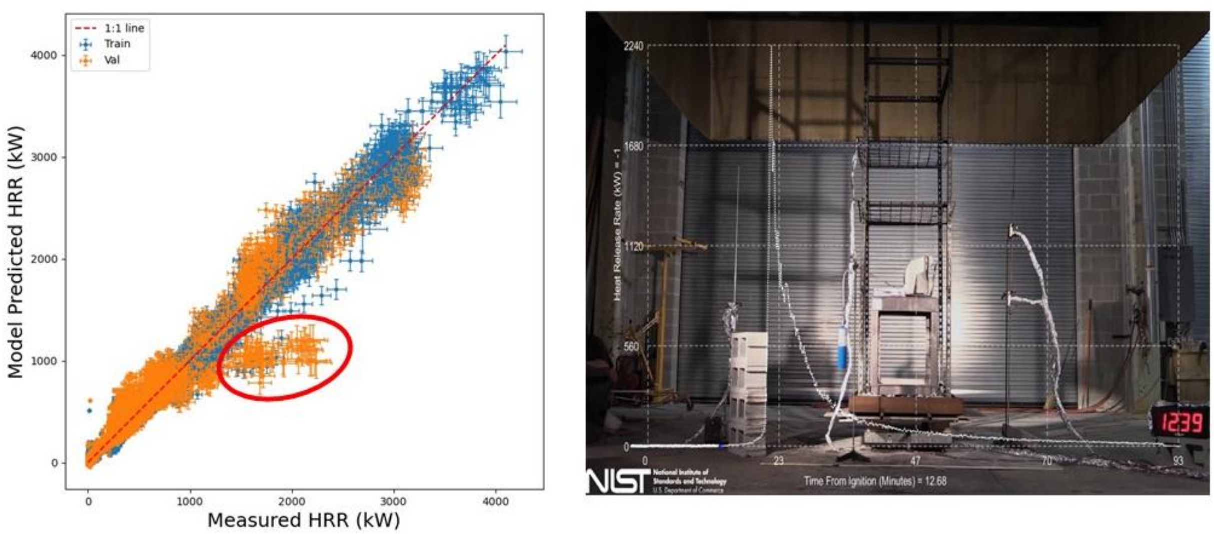

Figure 11. Left sub-figure shows the outlier frames marked by a red circle. All these frames were part of a single experiment in which a laptop / printer placed on a plastic work cart was burnt.

R2 scores for the training set was 0.99, while that for the validation set for 0.94 as shown in Table 6. Since the only input required to generate predictions from the neural network model is the video data, the trained and validated model can be extended to predict heat release rate for outdoor fires as well.

Table 6. Summary table for all the expeirments that were part of the current analysis

	# of frames (exp)	Loss	MAE (kW)	R2 score
Train	9602 (117)	1356	49	0.99
Val	3708 (30)	5761	100	0.94

4. Image Calorimetry: Impact and Conclusions

Heat release rate data is usually not available for outdoor fire experiments. This report bridges that gap by developing and demonstrating the use of a neural network technique to estimate HRR from fire video data. This novel technique termed as "image calorimetry" uses fire video data and a neural network technique to predict HRR.

The neural network model learns from select experiments (training set) that were part of the NIST Fire Calorimetry Database (FCD). The trained neural network model was subsequently used to predict the time dependent HRR for the experiments that were part of the validation set. A total of 147 experiments involving 13,310 images were analyzed. These experiments were part of the "Transient Combustibles 2018" and "Multiple Item Transient Combustibles 2020" projects in the FCD database. Even though the FCD is a nice database, it is a very limited one in many regards. For the model to be used in a more general manner, the training should be performed on a larger database of experiments with diverse fire scenarios, light conditions and camera settings.

Results presented in this paper show good comparison with the time dependent measured HRR with an overall accuracy score of 0.93. Our model is based on a recurrent neural network to analyze a sequence of images that are part of video, instead of looking at individual images only. The image calorimetry approach presented in this paper would improve fire measurement science through the development of a novel approach for estimating transient HRR from fire images and video, with application to outdoor fire experiments.

4.1. Image Calorimetry: Opportunities and Challenges

Heat release measurements are not available for outdoor fires since it is difficult to perform oxygen depletion calorimetry on such experiments. For such scenarios, availability of a trained neural network model will be critical for estimating heat release rate. Future work will involve using the model for real scale outdoor experiments. We plan to extend the analysis to "Vegetation Burn" experiment series, that are part of the FCD database.

It would be useful to understand the differences in model predictions for sooty and non-sooty fires. It is conceivable that the model could severely under-predict the true HRR for fires that are extremely sooty. Training the neural network models to learn from sooty and non-sooty fires can help in extending the model to sooty fires.

Using a single camera to obtain video data can be limiting for fire scenarios where the aspect ratio (ratio of breadth to width) is different from one. For example, if a single camera was looking at the short end of a line fire, the predicted HRR could be very small. An improvement to the model can be in using two or more cameras placed orthogonally to each other, instead of using just a single camera to obtain video data. Having multiple cameras provides the model critical information about the width and depth of the fire experiment, which can be completely missed by using a single camera.

The model can also be extended to other important parameters such as estimating soot yield. The proposed methodology is relatively general purpose and can be extended to other important fire parameters of interest. It can also be useful to add additional features to the model such as heat flux measurements, which can inform the model and improve model predictions.

The effect of camera lenses on the quality of the collected video data can influence model predictions. Similarly, the camera location, orientation, zoom and parallax can distort an image, leading to errors in the predicted HRR. Estimating the uncertainty introduced by these parameters is critical to fully understand the error bars in our predictions.

From the neural network point of view, further research is needed in the use of sequential models with highly non-uniform information distribution. Creating embeddings from the images that are rich in context will also help in reducing model over-fitting and reduce uncertainties in our predictions.

References

[1] Babrauskas V, Peacock RD (1991) Heat release rate: the simple most important variable in fire hazard. Fire Saf J 18:255‑272

[2] Quintiere J.G., Principles of Fire Behavior, 3rd Ed., CRC Press, 2016.

[3] Tewarson A., Heat release rate in fires, Fire Mater. 4 (1980) 185–191.

[4] Thornton W., The relation of oxygen to the heat of combustion of organic compounds, Philos. Mag. J. Sci. 33 (1917) 196–203.

[5] Biteau H., Steinhaus T., Schemel C., Simeoni A., Marlair G., Bal N., Calculation methods for the heat release rate of materials of unknown composition, Fire Saf. Sci. 9 (2008) 1165–1176.

[6] Standard Practice for Full-Scale Oxygen Consumption Calorimetry Fire Test, ASTM E2067-22, January 2022.

[7] Heskestad G. Fire plumes, flame height, and air entrainment. SFPE handbook of fire protection engineering. 5th ed. 2016.

[8] Carmignani, L., Flame Tracker: An image analysis program to measure flame characteristics, SoftwareX 15 (2021) 100791

[9] Gao Z, Ji J, Wan H, Li K, Sun J (2015) An investigation of the detailed flame shape and flame length under the ceiling of a channel. Proc Combust Inst 35:2657–2664

[10] Huang, X, Zhuo, X, Huang, T, Zheng, Z., Cheng, C., Chow, W., Simple flame height correlation for buoyancy-controlled diffusion plumes generated by rectangular sources fire different aspect ratios, Fuel 254 (2019) 115655.

[11] Tang F, Hu LH, Qiu ZW, et al. A global model of plume axial temperature profile transition from axisymmetric to line-source pool fires in normal and reduced pressures. Fuel 130 (2014) 211–4.

[12] Li, K., Mao, S. & Feng, R. Estimation of Heat Release Rate and Fuel Type of Circular Pool Fires Using Inverse Modelling Based on Image Recognition Technique. Fire Technol 55, 667–687 (2019).

[13] Ji J, Tan TT, Gao ZH, et al. Influence of sidewall and aspect ratio on burning behavior of rectangular ethanol and heptane pool fires. Fuel 2019;238:166–72.

[14] Linteris, G.T., Rafferty I.P., Flame size, heat release, and smoke points in material flammability, Fire Safety Journal 43 (2008) 442-450

[15] Ligang, Z., Minggao, Y., Suijun, Y., Chang, L., Measurement of Flame Height by Image Processing Method, Advanced Materials Research, Vol 301-303 (2011) pp. 983-988.

[16] Orloff L, de Ris J, Froude modeling of pool fires, Symp Combust 19:885–895, 1982

[17] Wong, A.K., Fong, N., Study of Pool Fire Heat Release Rate Using Video Fire Detection, International High Performance Buildings Conference, 2014.

[18] Omiotek, Z.; Kotyra, A, Flame Image Processing and Classification Using a Pre-Trained VGG16 Model in Combustion Diagnosis. Sensors 2021, 21, 500.

[19] Bonner, M. Wegrzynski, W., Rein, G., Visual Fire Power: An algorithm for Measuring Heat Release Rate of Visible Flames in Camera Footage with Applications in Façade Fire Experiments, Fire Technology, 59, 191-215, 2023

[20] Wang, Z. L., Zhang, T. H., & Huang, X. Y. (2023). Predicting real-time fire heat release rate by flame images and deep learning. Proceedings of the Combustion Institute, 39(3), 4115-4123. https://doi.org/10.1016/j.proci.2022.07.062

[21] Wang, Z. L., Tianhang, Z., Huang, X., Automatic real-time fire distance size and power measurement driven by stereo camera and deep learning, Fire Safety Journal, 140 (2023) 103981
[22] Evans, D. D., Madrzykowski, D., Haynes, G. A., Flame Heights and Heat Release Rates of 1991 Kuwait Oil Field Fires, Fire Safety Science – Proceedings of the Fourth International Symposium, pp. 1279-1289, 1994.
[23] Sivathanu, Y. R., Gore, J.P., Total Radiative Heat Loss in Jet Flames from Single Point Radiative Flux Measurements, Combustion and Flame, 94: 265-270, (1993).
[24] An Introduction to Statistical Learning, G. James, D. Witten, T. Hastie, R. Tibshirani, Springer, New York, 2013.
[25] NIST Fire Calorimetry Database, https://doi.org/10.18434/mds2-2314, 2021.
[26] LeCuhn, Yann, et al. "Gradient-based learning applied to document recognition", Proc of IEEE 86.11 (1998)
[27] Structure Separation Experiments: Shed Burns without Wind, https://doi.org/10.6028/NIST.TN.2235, 2022.

Appendix A. Case study of using Heskestad Equation to predict heat release rate

The NIST Fire Calorimetry Database (FCD), is an online public resource containing the results of fire experiments [1] conducted at the National Fire Research Laboratory (NFRL). The FCD consists of data augmented video, images, and transient heat release rate measurements (oxygen depletion calorimetry). In this section, the inverted form of the Heskestad correlation was used to estimate heat release rate from the fire images stored in the FCD database and the predictions were subsequently compared with the measured heat release rate (also available from the FCD).

We specifically focus on a calorimetry confirmation experiment with natural gas tube burner. This experiment has a name tag of "NGQC_9m_50kgs_8MW" and an ID "1583174916" stored in the FCD database. The left sub-figure of Figure 12 shows an image corresponding to the peak heat release rate value of 8454 kW as measured using oxygen depletion calorimetry. The inverted Heskestad correlation to estimate HRR requires an estimation of the fire height and diameter from this image. This can be accomplished by estimating size of the pixels, which in turn can be obtained by estimating the number of pixels in an object of known length. The tube gas burner shown in Figure 12 (right sub-figure) was used to estimate the size of the pixels.

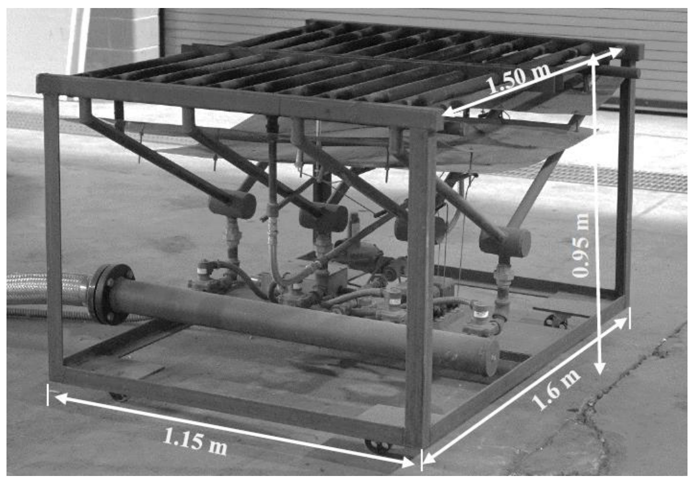

Figure 12 Left sub-figure shows an image corresponding to the peak heat release rate obtained from the calorimetry confirmation experiment (NGQC_9m_50kgs_8MW). The right sub-figure shows the dimensions of the 1.5 m tube gas burner that was used during the experiment.

Measurements were made both in the horizontal and vertical direction. In the horizontal direction, we estimated 175 pixels covering 1.15 m (top row of Table 7). The estimated HRR using the inverse Heskestad equation was 1801 kW, which is 79 % lower than the measured HRR of 8454 kW. In the vertical direction, we estimated 90 pixels covering 0.95 m (2nd row of Table 7). The estimated HRR was 4625 kW, which is 45 % lower than the measured HRR.

Measuring flame length and flame diameter from images is difficult and can result in large errors in the estimated HRR. Similar conclusions have been made by other author who have used images to estimate HRR using the Heskestad correlation [18]-[9]. There is clearly a need for a more robust method to estimate heat release rate.

Table 7. Estimation of flame length and flame diameter for the fire shown in Figure 12. The estimated HRR based on the inverse Heskestad correlation has been compared with measured HRR.

Estimated L (m)	Estimated D (m)	Estimated HRR (kW)	Measured HRR (kW)	% Error
3.54	1.15	1801	8454	79
5.70	1.15	4625	8454	45

A.1. More Challenging Cases

Figure 13 shows additional cases for which it is even more challenging to estimate heat release rate using the Heskestad correlation.

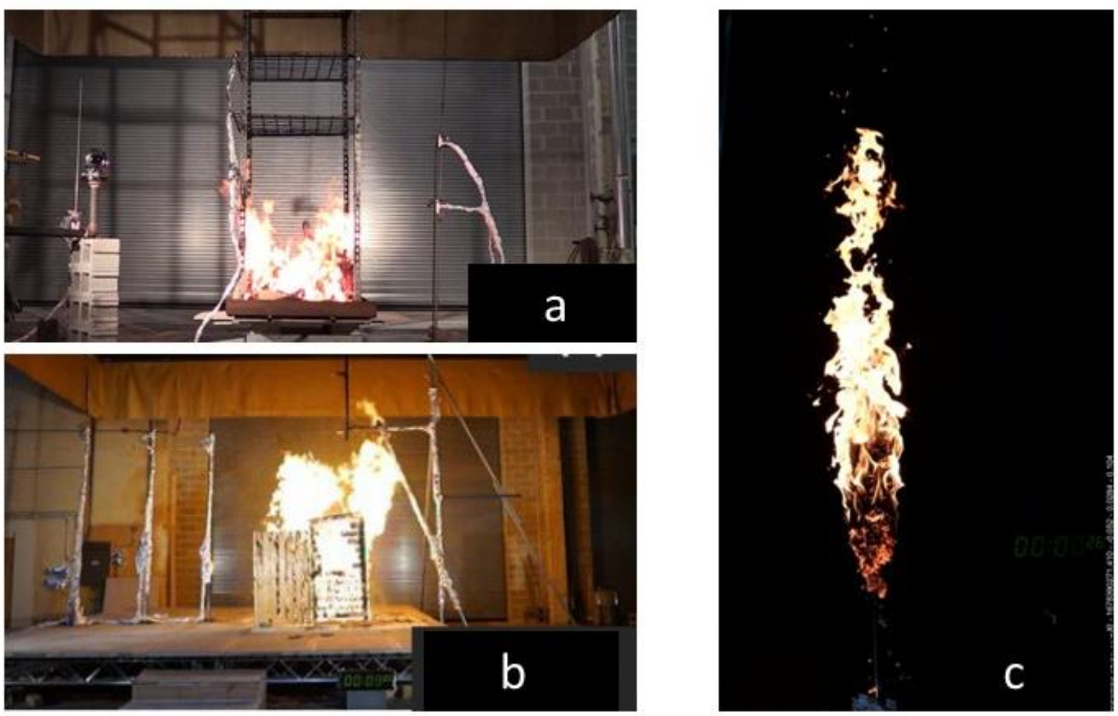

Figure 13. a) Image during burning of a plastic cart with fax, laptop, printer & binder (peak HRR 2502 +- 149 kW) b) Burning of very small shed with 6 cribs, 9 minutes after ignition [27], c) Image during burning of a small tree.

Figure 13a shows an image from burning of a plastic card with fax, laptop, printer and binder. During this experiment, a laptop and printer were put on the top level of a two-level plastic cart. Ignition occurs at the top level, followed by melt dripping onto the lower level, collapse of the top level and finally a fire that involves both the levels. For this scenario, it is very difficult to define the flame length or the flame width that can be used for Heskestad correlation.

Figure 13b shows burning of a very small shed with 6 cribs [27]. The image was taken approximately 9 minutes after ignition. Again, for this scenario, it is very challenging to define a flame length and a flame diameter, as there are multiple fires. Uncertainty in defining a flame length and flame diameter can result in uncertainty for estimating the heat release rate.

Finally, Figure 13c shows an image during the burning of a small tree, where defining a flame width and flame length can prove to be challenging. It is not clear if the flame width is the base of the tree or the widest portion of the image.

For all these scenarios, use of Heskestad correlation to estimate heat release rate can result in significant errors. The availability of a more accurate and robust technique for estimating heat release rate for such scenarios is the motivation for this research.